Cancer Management and Research

Dovepress

open access to scientific and medical research

Open Access Full Text Article

ORIGINAL RESEARCH

Circ_HIPK3 Knockdown Inhibits Cell Proliferation, Migration and Invasion of Cholangiocarcinoma Partly via Mediating the miR-148a-3p/ULK1 Pathway

Junning You[1]
Xiaolin Wang[2]

[1]Department of Emergency, Xianyang Hosptial, Yan'an University, XianYang, Shaanxi, People's Republic of China; [2]Department of General Surgery, Yulin No.2 Hospital, Yulin, Shaanxi, People's Republic of China

Background: The incidence of cholangiocarcinoma (CCA) is on the rise in recent years, and its pathogenesis may be associated with the dysregulation of circular RNAs (circRNAs). Hence, we aimed to investigate the role of circRNA homeodomain interacting protein kinase 3 (circ_HIPK3) in CCA.

Methods: The expression of circ_HIPK3, miR-148a-3p and unc-51 like kinase 3 (ULK1) mRNA was detected using quantitative real-time polymerase chain reaction (qPCR). The role of circ_HIPK3 in cell proliferation was detected by 3-[4, 5-dimethylthiazol-2-yl]-2, 5 diphenyl tetrazolium bromide (MTT) assay and colony formation assay. Cell apoptosis and cell cycle progression were investigated using flow cytometry assay. Cell migration and invasion were detected by transwell assay. The protein levels of ULK1 and migration/invasion-associated markers were measured using Western blot. The putative relationship between miR-148a-3p and circ_HIPK3 or ULK1 was validated by dual-luciferase reporter assay. The role of circ_HIPK3 was also investigated in vivo.

Results: Circ_HIPK3 was overexpressed in CCA tissues and cells. In function, circ_HIPK3 knockdown inhibited CCA cell proliferation, migration and invasion and induced apoptosis and cell cycle arrest. It was confirmed that miR-148a-3p was a target of circ_HIPK3, and ULK1 was a target of miR-148a-3p. Circ_HIPK3 regulated ULK1 expression by targeting miR-148a-3p. Rescue experiments showed that miR-148a-3p inhibition reversed the effects of circ_HIPK3 knockdown. Besides, miR-148a-3p enrichment-blocked cell proliferation, migration and invasion were recovered by ULK1 overexpression. In vivo, circ_HIPK3 knockdown inhibited solid tumor growth.

Conclusion: Circ_HIPK3 knockdown blocked CCA malignant development partly via regulating the miR-148a-3p/ULK1 pathway.

Keywords: circ_HIPK3, miR-148a-3p, ULK1, cholangiocarcinoma

Introduction

Cholangiocarcinoma (CCA), a biliary epithelial tumor, is classified into intrahepatic, perihilar and distal extrahepatic types in anatomy.[1] CCA is the second most common liver malignant tumor after hepatocellular carcinoma (HCC), accounting for 15–20% of primary liver tumors.[2,3] The prognosis of CCA is poor, with a median survival time less than 2 years and a survival rate less than 10%.[4] In addition, the incidence of CCA is increasing, especially in Western countries.[5] The main obstacles to CCA treatment are the firmness and early invasion of the tumor.[6] Unfortunately, even with surgical treatment, the recurrence rate of CCA is high

Correspondence: Xiaolin Wang
Tel +86-912-3362049
Email fuguren11@126.com

Received: 24 November 2020
Accepted: 2 March 2021
Published: 11 May 2021

(49–64%), and the 5-year survival rate of patients after resection is less than 45%.[6] The risk factors and molecular pathogenesis of CCA need to be further explored in order to identify markers conducive to early diagnosis and targeted therapy to improve patient survival.

Circular RNA (circRNA) is a group of non-coding RNAs (ncRNAs), characterized by a unique loop-closed structure. CircRNA is generally derived from the exon skipping of pre-mRNA transcription through back-splicing.[7] The function of circRNAs was underestimated in the past, and circRNAs arouse much attention recently due to the development of RNA sequencing technology. CircRNAs are involved in various cancers, with cell type-, tissue- and developmental stage-specific expression.[8] The abundance of circRNAs is more than ten times that of the corresponding linear mRNAs.[9] The stability of circRNAs is attributed to their structure, lacking free terminal ends.[10] Therefore, circRNAs are considered to be promising biomarkers for cancer treatment. In CCA, literature on the functions of circRNAs remains lacking, and some circRNAs, such as circ_0000284 and circ_0001649, have been reported to regulate CCA cell growth and metastasis.[11,12] Circ_0000284 is derived from homeodomain interacting protein kinase 3 (HIPK3) mRNA, also known as circ_HIPK3. However, its function is not fully understood in CCA.

Accumulating studies propose that circRNAs function as microRNAs (miRNAs) sponges and thus affect the expression and function of miRNA-targeted genes.[13] MiRNAs are a class of endogenous non-coding small RNAs that regulate the expression of tumor suppressor genes and oncogenes in cancer development.[14] MiR-148a-3p was reported to be involved in CCA development, associated with the inhibition of DNA methyltransferase-1 (DNMT-1).[15] Interestingly, it is predicted that miR-148a-3p is a target of circ_HIPK3 by bioinformatics tool. However, the interplay between miR-148a-3p and circ_HIPK3 in CCA is unclear. Unc-51 like kinase 1 (ULK1), a putative target of miR-148a-3p by bioinformatics prediction, is closed with tumorigenesis in various cancers.[16,17] The association between miR-148a-3p and ULK1 in CCA is also unknown and needs to be identified.

In the current study, we investigated the function of circ_HIPK3 on CCA cell proliferation, cycle, apoptosis, migration and invasion. We verified the relationship between miR-148a-3p and circ_HIPK3 or ULK1 and performed rescue experiments to demonstrate their interplays in CCA, aiming to provide a new insight into the understanding of CCA pathogenesis.

Materials and Methods

Tissue Collection and Study Approval

A total of 42 patients with CCA were recruited as subjects from Xianyang Hosptial, Yan'an University. The written informed consent was obtained from each subject, and then tumor tissues (n=42) and adjacent normal tissues (n=42) were surgically excised, frozen by liquid nitrogen and stored at −80°C conditions until use. The collection of tissues was conducted in accordance with the Declaration of Helsinki. Patients were diagnosed with CCA for the first time and confirmed by pathology with two pathologists, and patients with other cancers or previously underwent radiotherapy and chemotherapy were excluded in this study. This study was carried out with the approval of the Ethics Committee of Xianyang Hospital, Yan'an University.

Cell Line and Cell Culture

Two CCA cell lines, including RBE and HCCC-9810, and one human intrahepatic biliary epithelial cell line, HIBEpiC were purchased from Procell Co., Ltd (Wuhan, China). RBE and HCCC-9810 cells were cultured in RPMI1640 medium (Procell Co., Ltd.) containing 10% fetal bovine saline (FBS), and HIBEpiC cells were cultured in HIBEpiC specific complete medium (Procell Co., Ltd.) containing 10% FBS at a 37°C condition containing 5% CO_2.

Quantitative Real-Time Polymerase Chain Reaction (qPCR)

Total RNA from tissues and cells were extracted using the RNAiso Plus (Takara, Dalian, China) and then examined using NanoDrop 2000 (Thermo Fisher Scientific, Waltham, MA, USA). Then, the cDNA of circRNA and mRNA was synthesized using the Reverse Transcription Kit (Takara), and then cDNA was quantified using the SYBR Premix Ex Taq (Takara). The cDNA of miRNA was synthesized using the miRNA First-Strand Synthesis Kit (Clontech, Mountain View, CA, USA), and then cDNA was quantified using the miRNA qRT-PCR TB Green Kit (Clontech) under CFX96 System (Bio-Rad, Hercules, CA, USA). The relative expression was normalized by glyceraldehyde-3-phosphate dehydrogenase (GAPDH) or U6, using $2^{-\Delta\Delta ct}$ methods. The primer sequences were exhibited as follows:

circ_HIPK3, F: 5′-GATCCTGTTCGGCAGCCTTA-3′ and R: 5′-AGGCCATACCTGTAGTACCGA-3′; HIPK3, F: 5′-GACCTGAGGAGATCAAGCCG-3′ and R: 5′-ATTGGGGCCCATTCCTGAC-3′; miR-148a-3p,

F: 5′-TCAGTGCACTACAGAACTTTGT-3′ and R: 5′-GAATACCTCGGACCCTGC-3′; ULK1, F: 5′-AGATGTTCCAGCACCGTGAG-3′ and R: 5′-CACAGCTTGCACTTGGTGAC-3′; GAPDH, F: 5′-GCAAGTTCAACGGCACAG-3′ and R: 5′-ACGCCAGTAGACTCCACGAC-3′; U6, F: 5′-CTCGCTTCGGCAGCACATA-3′ and R: 5′-AACGATTCACGAATTTGCGT-3′;

Actinomycin D Treatment

RBE and HCCC-9810 cells were treated with Actinomycin D (1 μg/mL; MedChem Express, Monmouth Junction, NJ, USA). The treated cells were collected at different time points (0, 8, 16 and 24 h) and used for the detection of circ_HIPK3 expression and HIPK3 expression.

Cell Transfection

Small interference RNA (siRNA) targeting circ_HIPK3 (si-circ_HIPK3) and siRNA negative control (si-NC) were assembled by Genepharma (Shanghai, China). MiR-148a-3p mimic (miR-148a-3p), miR-148a-3p inhibitor (anti-miR-148a-3p) and mimic negative control (miR-NC), inhibitor negative control (anti-miR-NC) were purchased from Ribobio (Guangzhou, China). ULK1 sequence was cloned into pcDNA vector to form ULK1 overexpression plasmid (ULK1) was constructed by Genepharma, with pcDNA as a control. These oligonucleotides or plasmids were transfected into RBE and HCCC-9810 cells using Lipofectamine 3000 Transfection Reagent (Invitrogen, Carlsbad, CA, USA).

3-[4, 5-Dimethylthiazol-2-yl]-2, 5 Diphenyl Tetrazolium Bromide (MTT) Assay

The experimental cells were seeded into a 96-well plate at a density of 2×10^3 cells per well and cultured at the suitable conditions. MTT reagent (Sigma-Aldrich, St. Louis, MO, USA) was added into each well at the indicated time points (0, 24, 48 and 72 h), incubating for another 2 h. Next, dimethylsulfoxide (DMSO; Sigma-Aldrich) was added to completely dissolve formazan. The absorbance at 570 nm was examined using a microplate reader (Thermo Fisher Scientific, Waltham, MA, USA) to assess cell viability. This experiment was made in triplicate.

Flow Cytometry Assay for Cell Cycle and Cell Apoptosis

Cell cycle was analyzed using a Cell Cycle Analysis Kit (Beyotime, Shanghai, China). The experimental cells were collected, treated with trypsin and washed with pre-cold phosphate-buffered saline (PBS). Cells suspended in PBS were fixed using 70% ethanol at 4°C overnight. Subsequently, cells were washed with PBS and then stained with propidium iodide (PI) buffer (mixing with RNase A), incubating for 30 min at 37°C in the dark. The apoptotic cells were distinguished by flow cytometry (BD Bioscience, SanJose, CA, USA).

Cell apoptosis was monitored using Annexin V-FITC Apoptosis Detection Kit (Beyotime). In brief, the experimental cells were collected, treated with trypsin and washed with PBS. Then cells were resuspended in 195 μL binding buffer at a density of 4×10^5 cells/mL, followed by the addition of 5 μL Annexin V-FITC. Subsequently, cells were stained with 10 μL PI solution for 20 min at room temperature in the dark. The apoptotic cells were distinguished by flow cytometry (BD Bioscience).

Colony Formation Assay

The experimental cells were seeded into a 6-well plate at a density of 200 cells/well and then cultured in 37°C incubator supplemented with 5% CO_2 to allow colony growth. After culturing for two weeks, the colony surface was rinsed with PBS, fixed using 4% paraformaldehyde and stained with 0.1% crystal violet (Beyotime). The number of colonies was investigated under a microscope (Olympus, Tokyo, Japan).

Transwell Assay

Transwell chambers (BD Bioscience) were used to perform transwell assay to monitor cell migration and cell invasion. Transwell chambers were pre-coated with Matrigel (BD Bioscience) for invasion assay or with nothing for migration assay. The experimental cells were resuspended in serum-free culture medium were added into the upper chambers, and culture medium containing 10% FBS was added into the lower chambers to induce cell migration or invasion. After 24 h, cells migrated or invaded to the lower surface were fixed using 4% paraformaldehyde and stained with 0.1% crystal violet (Beyotime). Five randomly selected regions were used for cell counting using a microscope (100×; Olympus).

Western Blot

Total protein isolated using RIPA buffer (Sigma-Aldrich) was separated by 12% SDS-PAGE. Then, the separated proteins were transferred onto a PVDF membrane (Sigma-Aldrich), followed by the incubation using Western Blocking Reagent (Sigma-Aldrich). Then, the protein-stained membranes were probed with the primary antibodies, including anti-Snail (ab53519; Abcam, Cambridge, MA, USA), anti-E-cadherin (ab1416; Abcam), anti-ULK1 (ab179458; Abcam) and anti-GAPDH (ab8245; Abcam), followed by the incubation with the secondary antibody (ab205719; Abcam). Finally, the protein bands were presented using enhanced chemiluminescence (ECL) reagent (Beyotime).

Dual-Luciferase Reporter Assay

MiR-148a-3p was predicted as a target of circ_HIPK3 by bioinformatics tool starbase (http://starbase.sysu.edu.cn/), and ULK1 was predicted as a target of miR-148a-3p also by starbase. Their interaction was validated using dual-luciferase reporter assay. The mutant sequence fragments of circ_HIPK3 and ULK1 3′UTR (mutations at miR-148a-3p binding sites) were assembled. The wild-type sequence fragments of circ_HIPK3 and ULK1 3′UTR and the mutant sequence fragments of circ_HIPK3 and ULK1 3′UTR were cloned into pmiGLO reporter plasmid (Promega, Madison, WI, USA), including circ_HIPK3-WT, circ_HIPK3-MUT, ULK1-WT and ULK1-MUT. Then, the recombinant reporter plasmid was transfected with miR-148a-3p or miR-NC into RBE and HCCC-9810 cells. At 48 h post-transfection, the luciferase activity in cells was examined using the Dual-Luciferase Assay System (Promega) according to the protocol.

Xenograft Model

The animal study was approved by the Animal Care and Use Committee of Yanan Hosptial, Yan'an University and performed in accordance with the National Institutes of Health guide for the care and use of Laboratory animals. The experimental mice (Balb/c, female, 6–8 week old) were purchased from Beijing HFK Bioscience (Beijing, China) and housed at a pathogen-free condition. Short hairpin RNA (shRNA) targeting circ_HIPK3 (sh-circ_HIPK3) and shRNA negative control (sh-NC) were synthesized and packaged into lentiviral vector by Genepharma. We used HCCC-9810 cells to infect with lentiviral solution containing sh-circ_HIPK3 (n=5 per group) or sh-NC (n=5 per group) and subcutaneously injected HCCC-9810 cells into nude mice. Tumor was allowed to grow for 10 days, and then tumor volume (length×width^2×0.5) was measured every 5 days. After 30 days of tumor growth, the mice were killed. Tumor tissues were removed for the further experiments.

Statistical Analysis

All experiments were repeated three times. The differences were compared between two groups using Student's *t*-test. The differences among multiple groups were compared using analysis of variance (ANOVA) followed by Tukey's test for multiple test corrections. Data were processed using GraphPad Prism 8.0 software (GraphPad Prism, La Jolla, CA, USA) and presented as the mean ± standard deviation (S.D.). Correlation analysis was performed using Pearson correlation coefficient. *P* value less than 0.05 was considered to be statistically significant.

Results

Circ_HIPK3 Was Highly Expressed in CCA, and It Was Resistant to Actinomycin D

Initially, we monitored the expression level of circ_HIPK3 in CCA clinical tissues and cell lines. The difference was that circ_HIPK3 expression in tumor tissues (n=42) was significantly higher than that in normal tissues (n=42) (Figure 1A). Besides, circ_HIPK3 expression in RBE and HCCC-9810 cells was also notably higher than that in HIBEpiC cells (Figure 1B). Actinomycin D inhibited RNA polymerase II activity and total RNA synthesis. RBE and HCCC-9810 cells were treated with Actinomycin D for diverse time, and the data showed that Actinomycin D treatment significantly weakened the level of linear HIPK3 mRNA but hardly affected the level of circ_HIPK3 (Figure 1C and D), suggesting that circ_HIPK3 was far stable than linear molecules. The dysregulation of circ_HIPK3 hinted that circ_HIPK3 was involved in CCA progression.

Circ_HIPK3 Knockdown Inhibited CCA Cell Proliferation, Migration and Invasion

The endogenous level of circ_HIPK3 was lessened using si-circ_HIPK3 to explore the function of circ_HIPK3. The expression of circ_HIPK3 was strikingly decreased in RBE and HCCC-9810 cells after si-circ_HIPK3 transfection compared to si-NC, while the expression of linear HIPK3 was not changed (Figure 2A and B). MTT assay

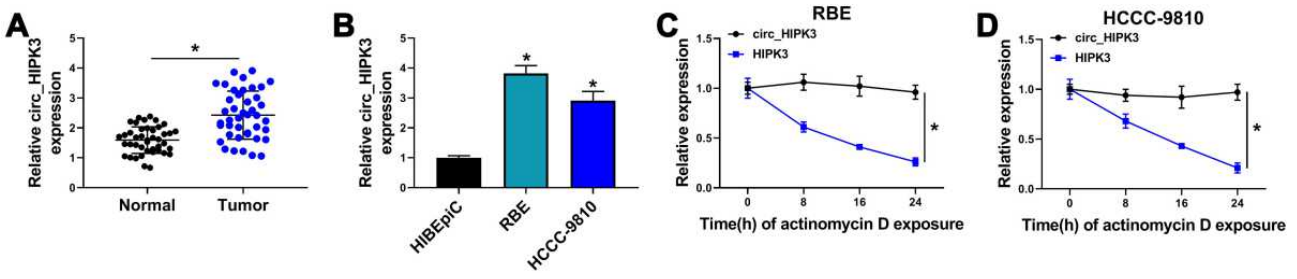

Figure 1 Circ_HIPK3 was upregulated in CCA tissues and cells. (**A**) The expression of circ_HIPK3 in tumor tissues (n=42) and normal tissues (n=42) was detected by qPCR (Student's *t*-test). (**B**) The expression of circ_HIPK3 in RBE, HCCC-9810 and HIBEpiC cells was detected by qPCR (ANOVA). (**C** and **D**) The stability of circ_HIPK3 and HIPK3 mRNA was identified using Actinomycin D (ANOVA). **P*<0.05.

showed that circ_HIPK3 knockdown notably inhibited cell proliferation (Figure 2C and D). Flow cytometry cell cycle assay introduced that circ_HIPK3 knockdown induced cell cycle arrest at the G0/G1 phase (Figure 2E and F). Colony formation assay presented that circ_HIPK3 knockdown notably suppressed the capacity of colony formation in RBE and HCCC-9810 cells (Figure 2G). Flow cytometry cell apoptosis assay showed that circ_HIPK3 knockdown effectively induced RBE and HCCC-9810 cell apoptosis (Figure 2H). Transwell assay clearly uncovered that circ_HIPK3 knockdown largely weakened the number of migrated and invaded cells (Figure 2I and J). Snail, a repressor of E-cadherin in the process of epithelial-mesenchymal transition (EMT), facilitates cancer cell migration and invasion.[18] Herein, we monitored that circ_HIPK3 knockdown notably suppressed the level of Snail and thus promoted the level of E-cadherin in RBE and HCCC-9810 cells, also indicating that circ_HIPK3 knockdown blocked cell migration and invasion (Figure 2K and L). Overall, these data suggested that circ_HIPK3 knockdown inhibited CCA cell proliferation, migration and invasion.

MiR-148a-3p, a Target of circ_HIPK3, Was Downregulated in CCA Tissues and Cells

For mechanism analysis, we screened and verified the potential target miRNAs of circ_HIPK3. Bioinformatics analysis provided several target miRNAs of circ_HIPK3, including miR-148a-3p. The binding sites between miR-148a-3p and circ_HIPK3 were shown in Figure 3A. Their relationship was further verified by dual-luciferase reporter assay because the cotransfection of miR-148a-3p and circ_HIPK3-WT reporter plasmid significantly decreased the luciferase activity in RBE and HCCC-9810 cells (Figure 3B and C). Besides, the expression of miR-148a-3p was strikingly enhanced in RBE and HCCC-9810 cells transfected with si-circ_HIPK3 relative to si-NC (Figure 3D). Moreover, the expression of miR-148a-3p was notably decreased in CCA cell lines (RBE and HCCC-9810) and tumor tissues (n=42) compared to non-cancer cell line (HIBEpiC) and normal tissues (n=42), respectively (Figure 3E and F). MiR-148a-3p expression was negatively correlated with circ_HIPK3 expression in these tumor tissues (Figure 3G).

Circ_HIPK3 Knockdown Inhibited CCA Cell Proliferation, Migration and Invasion by Increasing the Expression of miR-148a-3p

We performed rescue experiments to explore whether circ_HIPK3 affected CCA cell behaviors by mediating miR-148a-3p. The experimental cells were transfected with si-circ_HIPK3, si-NC, si-circ_HIPK3+anti-miR-148a-3p or si-circ_HIPK3+anti-miR-NC. The expression of miR-148a-3p was increased in cells transfected with si-circ_HIPK3 but largely repressed in cells transfected with si-circ_HIPK3+anti-miR-148a-3p (Figure 4A). MTT assay presented that si-circ_HIPK3 transfection-blocked cell proliferation was partly recovered by si-circ_HIPK3+anti-miR-148a-3p transfection (Figure 4B and C). Flow cytometry cell cycle arrest showed that si-circ_HIPK3 transfection-induced cell cycle arrest was largely alleviated by si-circ_HIPK3+anti-miR-148a-3p transfection (Figure 4D and E). Besides, colony formation ability was attenuated by si-circ_HIPK3 but recovered by si-circ_HIPK3+anti-miR-148a-3p in RBE and HCCC-980 cells (Figure 4F). Flow cytometry cell apoptosis assay introduced that the apoptotic rate promoted by circ_HIPK3 knockdown alone was largely suppressed by the

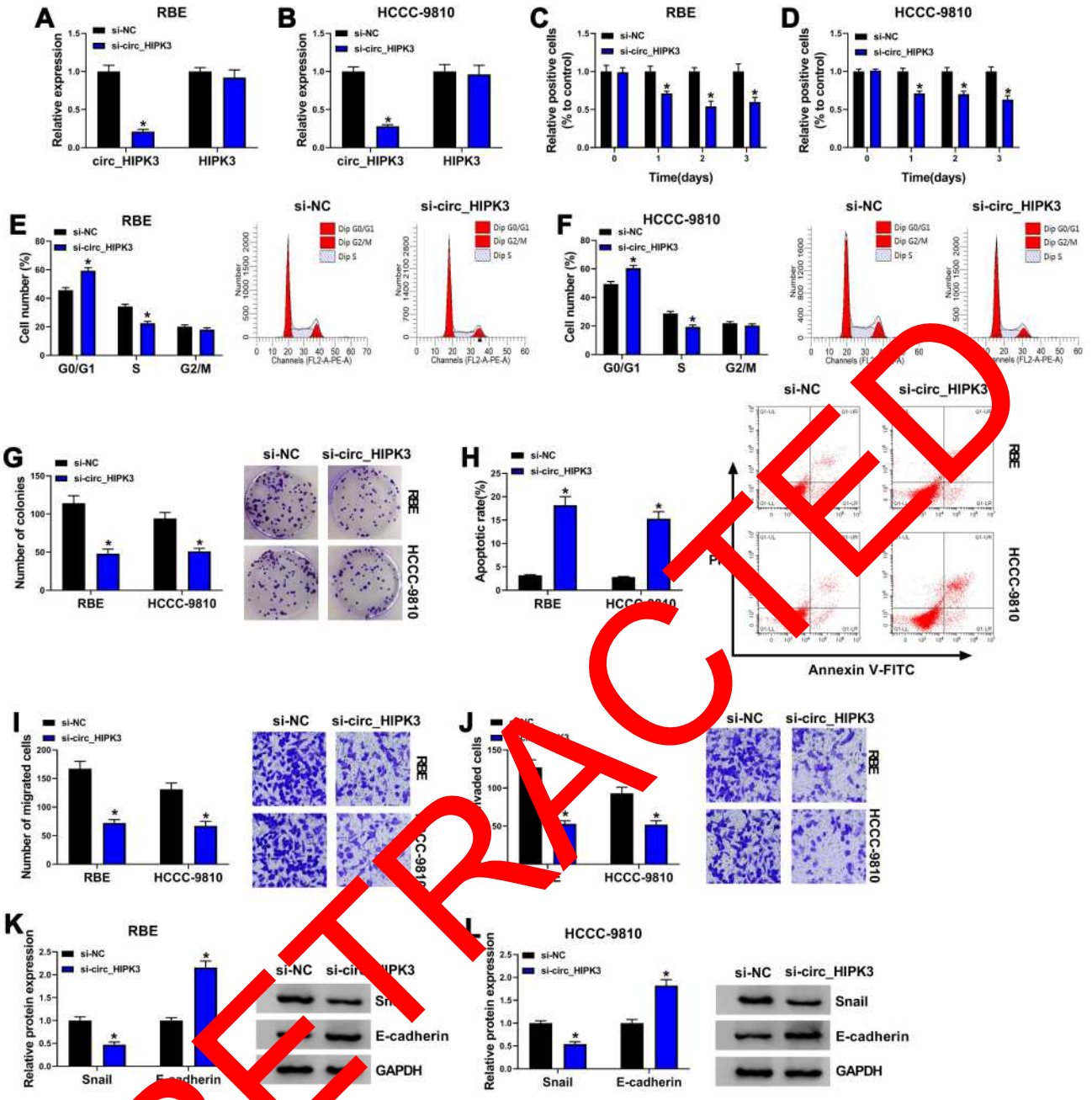

Figure 2 Circ_HIPK3 knockdown inhibited RBE and HCCC-9810 cell proliferation, migration and invasion. (**A** and **B**) The expression of circ_HIPK3 in RBE and HCCC-9810 cells after circ_HIPK3 knockdown was detected by qPCR (n=3, ANOVA). (**C** and **D**) The effect of circ_HIPK3 knockdown on cell proliferation was assessed by MTT assay (n=3, ANOVA). (**E** and **F**) The effect of circ_HIPK3 knockdown on cell cycle was assessed by flow cytometry assay (n=3, ANOVA). (**G**) The effect of circ_HIPK3 knockdown on cell proliferation was also assessed by colony formation assay (n=3, ANOVA). (**H**) The effect of circ_HIPK3 knockdown on cell apoptosis was assessed by flow cytometry assay (n=3, ANOVA). (**I** and **J**) The effect of circ_HIPK3 knockdown on cell migration and invasion was assessed by transwell assay (n=3, ANOVA). (**K** and **L**) The protein levels of Snail and E-cadherin were quantified to assess cell migration and invasion (n=3, ANOVA). *P<0.05.

reintroduction of anti-miR-148a-3p (Figure 4G). Transwell assay displayed that the number of migrated and invaded cells was depleted in RBE and HCCC-9810 cells transfected with si-circ_HIPK3 alone but partly restored in cells transfected with si-circ_HIPK3+anti-miR-148a-3p (Figure 4H and I). Additionally, the level of Snail inhibited by circ_HIPK3 knockdown was recovered by the additional miR-148a-3p inhibition, while the level of E-cadherin reinforced by circ_HIPK3 knockdown was blocked by the additional miR-148a-3p inhibition (Figure 4J and K). The data clearly showed that miR-148a-3p inhibition reversed the effects of circ_HIPK3 knockdown.

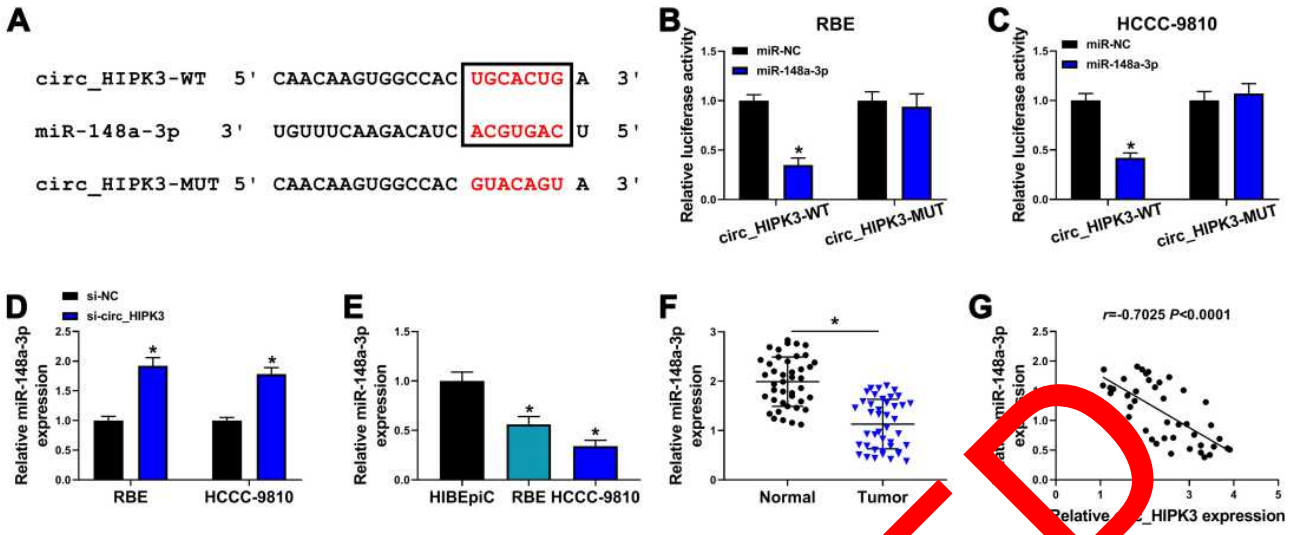

Figure 3 MiR-148a-3p was a target of circ_HIPK3. (**A**) The binding site between circ_HIPK3 and miR-148a-3p was analyzed by starbase. (**B** and **C**) The relationship between circ_HIPK3 and miR-148a-3p was validated by dual-luciferase reporter assay (n=3, ANOVA). (**D**) The expression of miR-148a-3p in RBE and HCCC-9810 cells transfected with si-circ_HIPK3 or si-NC was detected by qPCR (n=3, ANOVA). (**E**) The expression of miR-148a-3p in HIBEpiC, RBE and HCCC-9810 cells was detected by qPCR (n=3, ANOVA). (**F**) The expression of miR-148a-3p in CCA tumor tissues (n=42) and normal tissues (n=42) was detected by qPCR (Student's *t*-test). (**G**) The correlation between miR-148a-3p expression and circ_HIPK3 expression was analyzed by Pearson correlation coefficient. *P

ULK1, a Target of miR-148a-3p, Was Upregulated in CCA Tissues and Cells

For mechanism analysis, we further investigated the potential target mRNAs of miR-148a-3p. ULK1 was a p[redicted] target of miR-148a-3p, with special binding sites between its 3′UTR and miR-148a-3p sequence (Figure 5A). This relationship was validated by dual-luciferase reporter assay, and we found that the cotransfection of miR-148a-3p and ULK1-WT reporter plasmid notably diminished the luciferase activity in RBE and HCCC-9810 cells (Figure 5B and C). The expression of miR-148a-3p was strikingly increased in RBE and HCCC-9810 cells transfected with miR-148a-3p compared to miR-NC but strikingly declined in cells transfected with anti-miR-148a-3p compared to anti-miR-NC (Figure 5D), while the expression of ULK1 was markedly impaired in RBE and HCCC-9810 cells transfected with miR-148a-3p but strikingly elevated in cells transfected with anti-miR-148a-3p at mRNA and protein levels (Figure 5E and F). The data from qPCR and Western blot showed that ULK1 expression was notably higher in CCA tumor tissues compared to normal tissues (Figure 5G and H). ULK1 mRNA level was negatively correlated with miR-148a-3p level but was positively correlated with circ_HIPK3 level in these tumor tissues (Figure 5I and J). Also, the expression of ULK1 was notably elevated in RBE and HCCC-9810 cells compared to HIBEpiC cells by qPCR and Western blot analyses (Figure 5K and L). Moreover, we found that the expression of ULK1 was remarkably decreased in RBE and HCCC-9810 cells transfected with si-circ_HIPK3 compared to si-NC, while the expression of ULK1 was remarkably reinforced in RBE and HCCC-9810 cells transfected with si-circ_HIPK3+anti-miR-148a-3p compared to si-circ_HIPK3+anti-miR-NC (Figure 5M and N). The data indicated that circ_HIPK3 regulated the expression of ULK1 by mediating miR-148a-3p expression.

MiR-148a-3p Enrichment Suppressed CCA Cell Proliferation, Migration and Invasion by Decreasing ULK1 Level

To further explore the interplay between miR-148a-3p and ULK1 in CCA cell behaviors, RBE and HCCC-9810 cells were transfected with miR-148a-3p or miR-148a-3p+ULK1, with miR-NC or miR-148a-3p+pcDNA as the control. The expression of ULK1 was markedly depleted in RBE and HCCC-9810 cells transfected with miR-148a-3p but largely recovered in cells transfected with miR-148a-3p+ULK1 (Figure 6A and B). These experimental cells were available and used for the following assays. MTT assay showed that cell proliferation was strikingly inhibited in cells transfected with miR-148a-3p alone but partly promoted in cells transfected with miR-148a-3p+ULK1 (Figure 6C and D). Flow cytometry cell cycle assay exhibited that miR-148a-3p enrichment significantly induced RBE and HCCC-9810 cell cycle arrest, while ULK1 reintroduction largely relieved

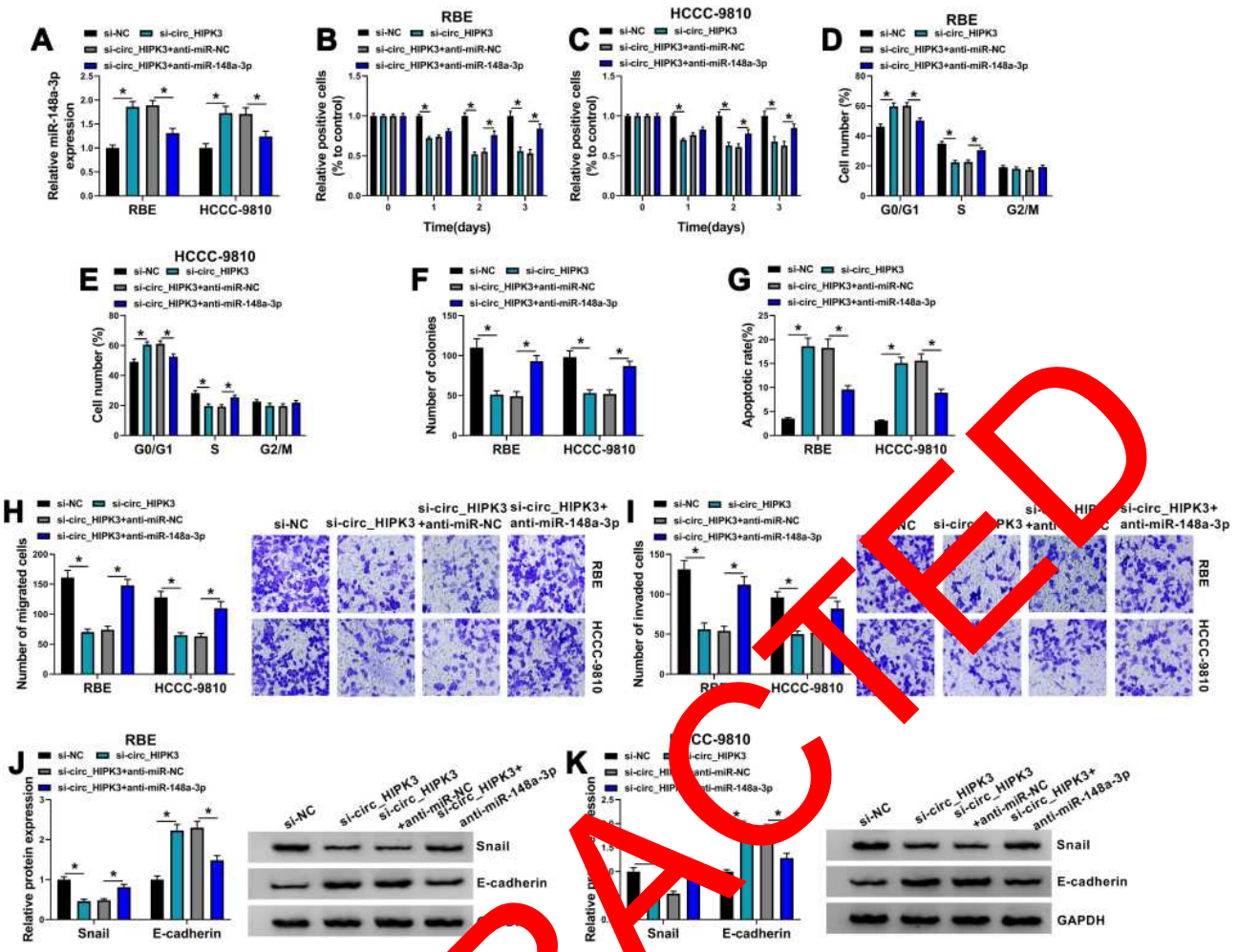

Figure 4 Circ_HIPK3 knockdown inhibited RBE and HCCC-9810 cell p[illegible]migration and invasion by enriching miR-148a-3p. (**A**) The expression of miR-148a-3p in RBE and HCCC-9810 cells transfected with si-circ_HIPK3, si-[illegible]c_HIPK3+anti-miR-148a-3p or si-circ_HIPK3+anti-miR-NC was detected by qPCR (n=3, ANOVA). In these transfected cells, (**B** and **C**) cell proliferation was examined using MTT assay (n=3, ANOVA). (**D** and **E**) Cell cycle was investigated using flow cytometry assay (n=3, ANOVA). (**F**) Cell proliferation was also assessed by colony formation assay (n=3, ANOVA). (**G**) Cell apoptosis was examined using flow cytometry assay (n=3, ANOVA). (**H** and **I**) Cell migration and cell invasion were examined using transwell assay (n=3, ANOVA). (**J** and **K**) The protein levels of Snail and E-cadherin were quantified by Western blot to assess cell migration and invasion (n=3, ANOVA). *P<0.05.

cell cycle arrest (Figure 6E and F). Colony formation assay showed that miR-148a-3p notably frustrated colony formation ability, while ULK1 reproduction recovered colony formation ability (Figure 6G). Flow cytometry cell apoptosis assay revealed that the apoptotic rate of RBE and HCCC-9810 cells induced by miR-148a-3p enrichment was suppressed by the reproduction of ULK1 (Figure 6H). Transwell assay showed that cell migration and invasion were significantly blocked in RBE and HCCC-9810 cells transfected with miR-148a-3p but notably recovered in cells transfected with miR-148a-3p+ULK1 (Figure 6I and J). In addition, the level of Snail was inhibited by miR-148a-3p transfection alone but recovered by miR-148a-3p+ULK1 transfection, while the level of E-cadherin was stimulated by miR-148a-3p transfection alone but repressed by miR-148a-3p+ULK1 transfection in RBE and HCCC-9810 cells (Figure 6K and L). These data suggested that miR-148a-3p enrichment blocked ULK1 expression and thus inhibited CCA cell proliferation, migration and invasion.

Circ_HIPK3 Knockdown Decelerated Tumor Growth in Mice

The role of circ_HIPK3 in CCA was further explored using Xenograft model. HCCC-9810 cells with sh-circ_HIPK3 led to lower tumor volume in nude mice compared to sh-NC (Figure 7A). The average weight of mice in each group was shown in Figure S1. Besides, HCCC-9810 cells with sh-circ_HIPK3 led to lower tumor weight and tumor size (Figure 7B), suggesting that circ_HIPK3 knockdown inhibited tumor growth. Moreover, the expression of circ_HIPK3

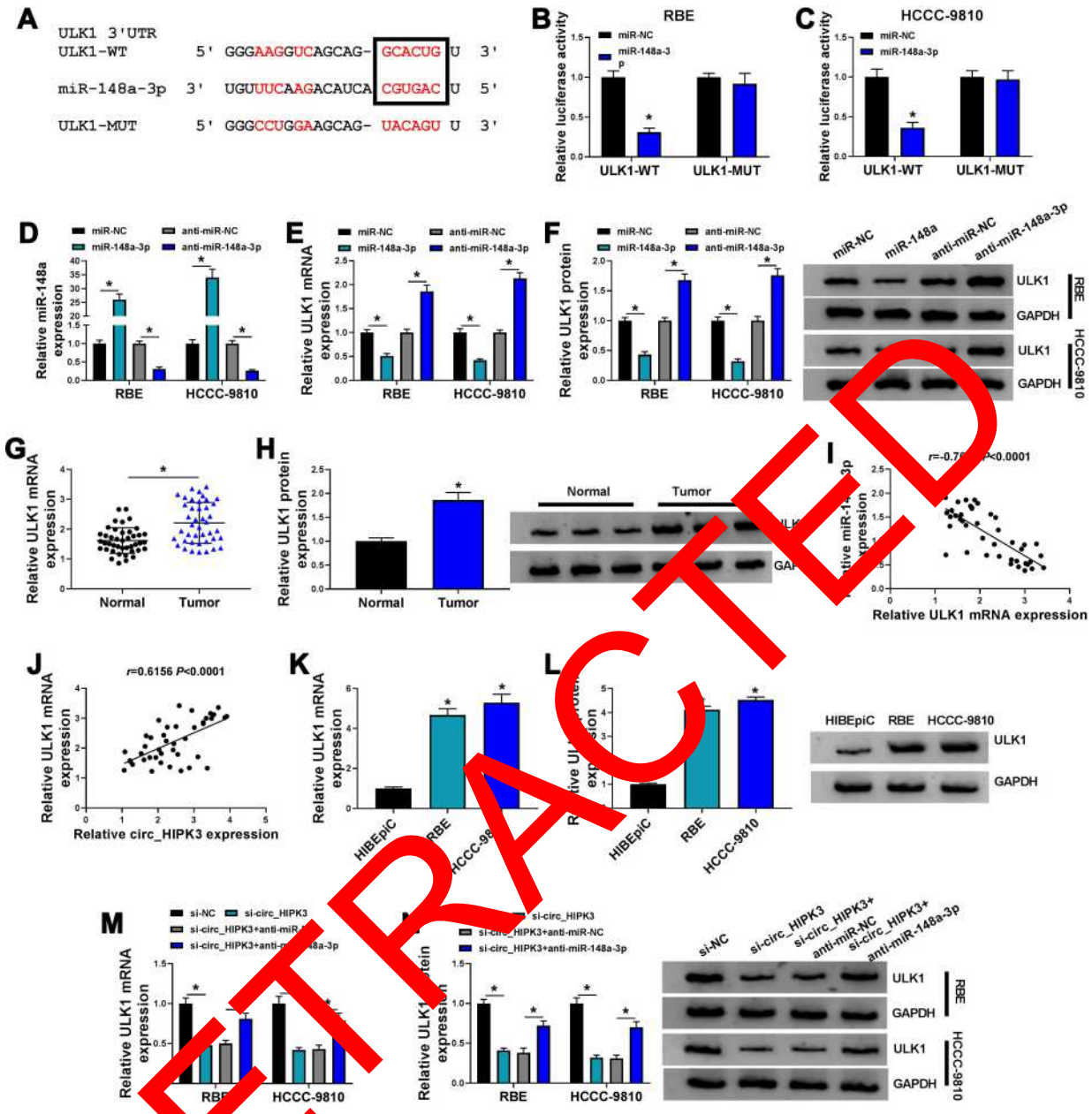

Figure 5 Circ_HI[illegible]gulated [illegible] expressi[illegible] of ULK1, a target of miR-148a-3p, by targeting miR-148a-3p. (**A**) The binding sites between ULK1 3′UTR and miR-148a-3p were analyzed [illegible] starba[illegible] (**B** and [illegible] The [illegible]tionship between ULK1 and miR-148a-3p was validated by dual-luciferase reporter assay (n=3, ANOVA). (**D**) The expression of miR-148[illegible]p in RBE [illegible]d HCCC-98[illegible] cells after miR-148a-3p or anti-miR-148a-3p transfection was measured by qPCR (n=3, ANOVA). (**E** and **F**) The expression of ULK1 in [illegible] and HC[illegible] cells after miR-148a-3p or anti-miR-148a-3p transfection was measured by qPCR and Western blot (n=3, ANOVA). (**G** and **H**) The expression o[illegible]K[illegible] CCA tumo[illegible] tissues (n=42) and normal tissues (n=42) was measured by qPCR and Western blot (Student's *t*-test). (**I** and **J**) The correlation between ULK1 expressio[illegible]d miR-148a-3p expression or circ_HIPK3 expression in CCA tissues was analyzed by Pearson correlation coefficient. (**K** and **L**) The expression of ULK1 in HIBEpiC, RBE a[illegible] HCCC-9810 cells was measured by qPCR and Western blot (n=3, ANOVA). (**M** and **N**) The expression of ULK1 in RBE and HCCC-9810 cells transfected with si-circ[illegible]IPK3, si-NC, si-circ_HIPK3+anti-miR-148a-3p or si-circ_HIPK3+anti-miR-NC was measured by qPCR and Western blot (n=3, ANOVA). **P*<0.05.

was strikingly decreased in sh-circ_HIPK3-injected tumor tissues by qPCR analysis (Figure 7C). The expression of miR-148a-3p was strikingly enhanced in tumor tissues from the sh-circ_HIPK3 group by qPCR analysis (Figure 7D). The expression of ULK1 was strikingly impaired in tumor tissues from the sh-circ_HIPK3 group by qPCR and Western blot analyses (Figure 7E and F). The data suggested that circ_HIPK3 knockdown inhibited tumor growth by suppressing ULK1 level via enriching miR-148a-3p level.

Discussion

In the present study, we focused on circ_HIPK3 whose expression level was aberrantly elevated in CCA tissues and cells. We used siRNA to mediate circ_HIPK3

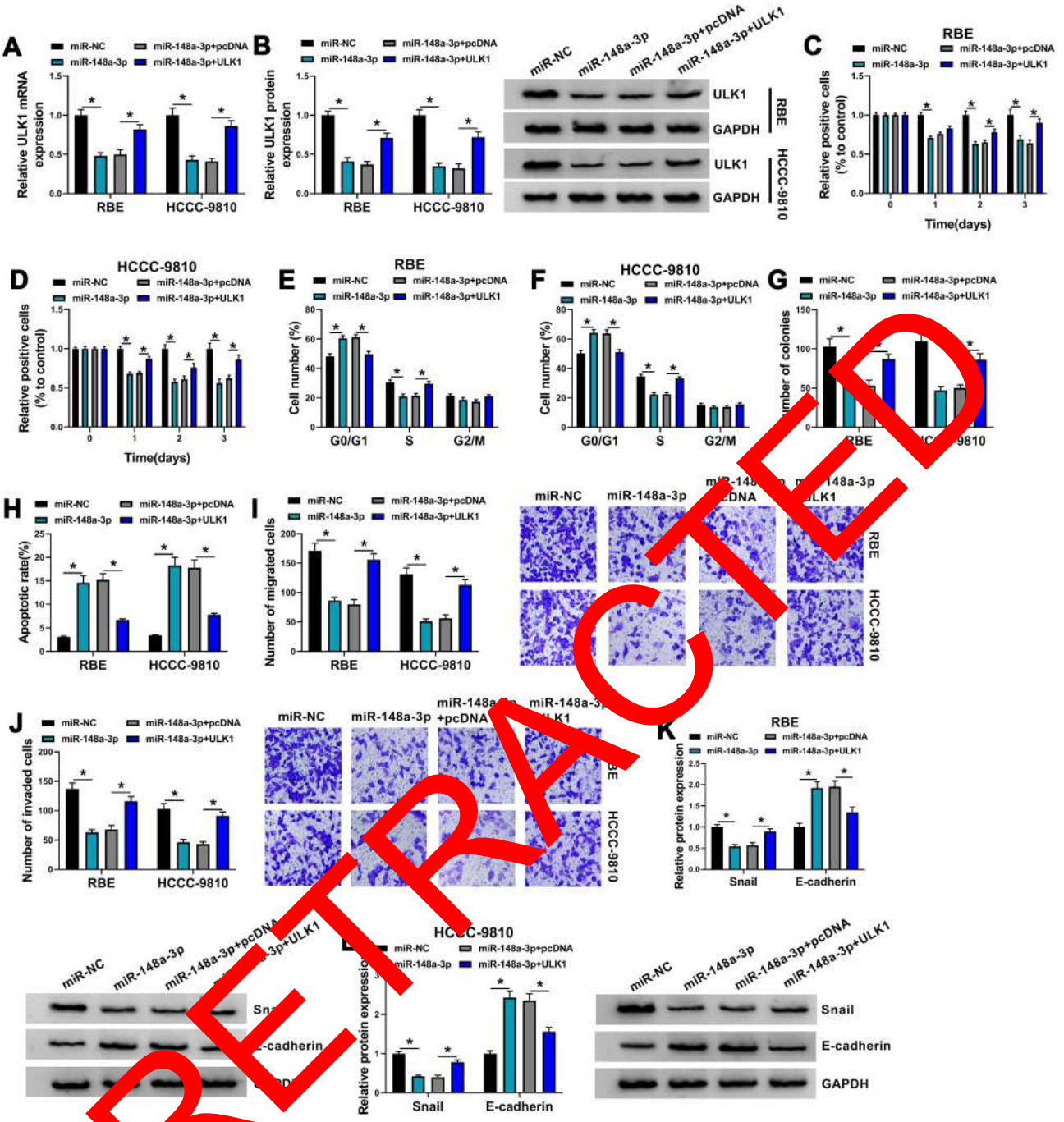

Figure 6 MiR-148a-3p inhibited RBE and HCCC-9810 cell proliferation, migration and invasion by targeting ULK1. (**A** and **B**) The expression of ULK1 in RBE and HCCC-9810 cells transfected with miR-148a-3p, miR-NC, miR-148a-3p+ULK1 or miR-148a-3p+pcDNA was measured by qPCR and Western blot (n=3, ANOVA). (**C** and **D**) Cell proliferation in these transfected cells was detected by MTT assay (n=3, ANOVA). (**E** and **F**) Cell cycle in these transfected cells was monitored using flow cytometry assay (n=3, ANOVA). (**G**) Cell proliferation in these transfected cells was also assessed by colony formation assay (n=3, ANOVA). (**H**) Cell apoptosis in these transfected cells was monitored by flow cytometry assay (n=3, ANOVA). (**I** and **J**) Cell migration and cell invasion in these transfected cells were monitored using transwell assay (n=3, ANOVA). (**K** and **L**) The protein levels of Snail and E-cadherin in these transfected cells were quantified by Western blot (n=3, ANOVA). *P<0.05.

knockdown to explore the functional role of circ_HIPK3 and found that circ_HIPK3 knockdown inhibited CCA cell proliferation, migration and invasion. For mechanism analysis, miR-148a-3p was discovered to be a target of circ_HIPK3, and ULK1 was a target of miR-148a-3p. Importantly, we noticed that circ_HIPK3 positively regulated ULK1 expression by competitively binding to miR-148a-3p, which was specially elucidated by rescue

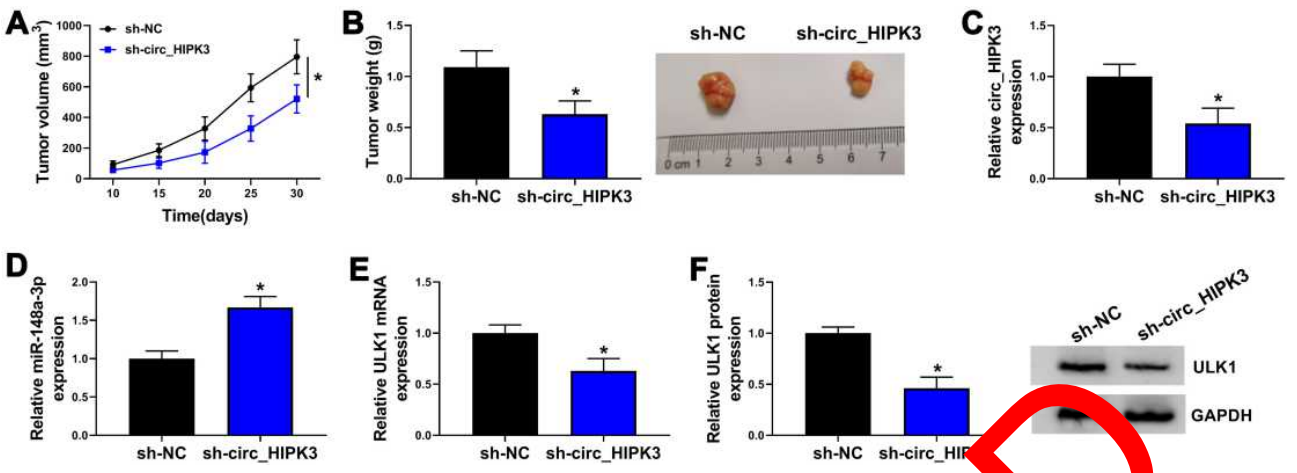

Figure 7 Circ_HIPK3 knockdown inhibited tumor growth in vivo. (**A**) HCCC-9810 cells harboring sh-circ_HIPK3 or sh-NC were injected into nude mice, and tumor volume was measured every 5 days from 10th day post-injection (ANOVA). (**B**) Tumor weight was measured after 30 days (Student's *t*-test). (**C**) The expression of circ_HIPK3 in the excised tissues was detected by qPCR (Student's *t*-test). (**D**) The expression of miR-148a-3p in the excised tissues was detected by qPCR (Student's *t*-test). (**E** and **F**) The expression of ULK1 in the excised tissues was detected by qPCR and Western blot (Student's *t*-test). *P<0.05.

experiments. Moreover, the oncogenic effect of circ_HIPK3 was also verified in vivo by animal study. All of our findings contributed to the understanding the pathogenesis of CCA.

CircRNAs have developed into research hotspots in various cancers, including CCA. A growing body of literature has revealed the role of certain circRNA in CCA and provided some promising biomarkers to predict CCA treatment and outcomes. For instance, circ_0001230 was upregulated in CCA, and its expression was associated with clinical severity. Circ_0005230 overexpression accelerated CCA cell growth and metastatic properties, thus aggravating CCA development.[12] On the contrary, circ_0001649 was notably downregulated in CCA tissues and cells, and circ_0001649 overexpression notably impaired CCA cell proliferation, migration and invasion.[12] Circ_0000284 (circ_HIPK3) is a splicing variant of HIPK3 mRNA, with multiple biological functions in cancer progression. It was reported that circ_HIPK3 functioned as an oncogene to promote cell proliferation, migration and tumorigenesis in non-small cell lung cancer and glioma.[20,21] In CCA, Wang et al. reported that circ_HIPK3 expression was increased in CCA cell lines, tissues and plasma exosomes, and forced expression of circ_0000284 promoted the abilities of CCA cell proliferation, migration and invasion.[11] These studies documented the partial functions of circ_HIPK3 in various cancers and proposed that circ_HIPK3 was an oncogenic driver. Largely consistent with these findings, we performed MTT assay and colony formation assay and found that circ_HIPK3 knockdown inhibited CCA cell proliferation and colony formation ability. Flow cytometry assay showed that circ_HIPK3 knockdown promoted CCA cell cycle arrest and apoptosis. Transwell assay showed that circ_HIPK3 knockdown blocked CCA cell migration and invasion. These assays highlighted that circ_HIPK3 knockdown inhibited CCA cell growth and metastasis. However, the regulatory mechanisms of circ_HIPK3 were still not fully understood in CCA. Innovatively, we investigated the potential target miRNAs of circ_HIPK3 to explore its functional mechanism.

As a result, miR-148a-3p was a putative target of circ_HIPK3 by bioinformatics analysis, which was further verified by dual-luciferase reporter assay. Overall the previous studies, miR-148a-3p functioned as a tumor suppressor and blocked the development of numerous cancers, such as bladder cancer and ovarian cancer.[22,23] Interestingly, miR-148a-3p expression was shown to be decreased in CCA cells, and miR-148a-3p downregulation was linked to anabatic intrahepatic CCA cell proliferation, migration and invasion, which was attributed to the increased expression of GLUT1, a target of miR-148a-3p.[15,24] Consistent with the idea from these studies, we noticed that miR-148a-3p expression was declined in CCA tissues and cells. The inhibition of miR-148a-3p reversed the effects of circ_HIPK3 knockdown, thus recovering circ_HIPK3 knockdown-inhibited CCA cell proliferation, migration and invasion, while miR-148a-3p overexpression noticeably suppressed these malignant cell phenotypes.

Previous studies have elucidated that miR-148a-3p participates in cancer processes partly by mediating its target genes.[22,24] However, there are numerous potential genes targeted by miR-148a-3p that have not been verified. Herein, we proposed that ULK1 was a novel target of miR-148a-3p, which was validated by dual-luciferase reporter assay. Rescue experiments presented that ULK1 overexpression recovered miR-148a-3p-inhibited proliferation, migration and invasion of CCA cells. Previous papers harbored the view that targeted inhibition of ULK1 contributed to the inhibition of tumor growth and metastasis in diverse cancers.[25–27] In CCA, it was documented that ULK1, targeted by miR-373, suppressed CCA cell apoptosis and promoted autophagy, thus promoting CCA development.[28] These views expressed that ULK1 was an oncogene in different cancers, suggesting that ULK1 inhibition might play the same effects with circ_HIPK3 knockdown. Interestingly, our findings showed that ULK1 expression was negatively correlated with miR-148a-3p expression but positively correlated with circ_HIPK3 expression in CCA tissues, and ULK1 expression was impaired in CCA cells after circ_HIPK3 knockdown but recovered after miR-148a-3p inhibition, suggesting that ULK1 was involved in the circ_HIPK3/miR-148a-3p network.

In conclusion, circ_HIPK3 downregulation blocked CCA cell proliferation, migration and invasion partly by mediating the miR-148a-3p/ULK1 axis. Our study provided a CCA-associated circRNA and established the circ_HIPK3/miR-148a-3p/ULK1 network to further understand the mechanism of circ_HIPK3 action in CCA, which might be a theoretical basis for circ_HIPK3 as a biomarker in future treatment. Nonetheless, there were still limitations in this study. For example, the associated oncogenic signaling pathways were not investigated, and other downstream targets of miR-148a-3p were not identified. Further experiments need to be performed to solve these issues.

Highlights

1. Circ_HIPK3 is overexpressed in cholangiocarcinoma tissues and cells.
2. Circ_HIPK3 knockdown suppresses cholangiocarcinoma growth and tumorigenesis in vitro and in vivo.
3. Circ_HIPK3 regulates ULK1 expression by targeting miR-148a-3p.
4. Circ_HIPK3 regulates cholangiocarcinoma progression by modulating the miR-148a-3p/ULK1 pathway.

Data Sharing Statement

The analyzed data sets generated during the present study are available from the corresponding author on reasonable request.

Ethics Approval and Consent to Participate

The present study was approved by the ethical review committee of Xianyang Hosptial, Yan'an University. Written informed consent was obtained from all enrolled patients.

Consent for Publication

Patients agree to participate in this work.

Disclosure

The authors declare that they have no competing interests in this work.

References

1. Ilyas S, Gores GJ. Pathogenesis, diagnosis, and management of cholangiocarcinoma. *Gastroenterology*. 2013;145(6):1215–1229. doi:10.1053/j.gastro.2013.10.013
2. Blechacz B. Cholangiocarcinoma: current knowledge and new developments. *Gut Liver*. 2017;11(1):13–26. doi:10.5009/gnl15568
3. Rizvi S, Khan SA, Hallemeier CL,et al. Cholangiocarcinoma - evolving concepts and therapeutic strategies. *Nat Rev Clin Oncol*. 2018;15(2):95–111. doi:10.1038/nrclinonc.2017.157
4. Brito AF, Abrantes AM, Encarnação JC, et al. Cholangiocarcinoma: from molecular biology to treatment. *Med Oncol*. 2015;32(11):245. doi:10.1007/s12032-015-0692-x
5. Banales JM, Cardinale V, Carpino G,et al. Expert consensus document: cholangiocarcinoma: current knowledge and future perspectives consensus statement from the European Network for the Study of Cholangiocarcinoma (ENS-CCA). *Nat Rev Gastroenterol Hepatol*. 2016;13(5):261–280.
6. Brivio S, Cadamuro M, Fabris L, et al. Molecular mechanisms driving cholangiocarcinoma invasiveness: an overview. *Gene Expr*. 2018;18(1):31–50. doi:10.3727/105221617X15088670121925
7. Kelly S, Greenman C, Cook PR, et al. Exon skipping is correlated with exon circularization. *J Mol Biol*. 2015;427(15):2414–2417. doi:10.1016/j.jmb.2015.02.018
8. Salzman J, Chen RE, Olsen MN, et al. Cell-type specific features of circular RNA expression. *PLoS Genet*. 2013;9(9):e1003777. doi:10.1371/journal.pgen.1003777
9. Jeck WR, Sorrentino JA, Wang K, et al. Circular RNAs are abundant, conserved, and associated with ALU repeats. *RNA*. 2013;19(2):141–157. doi:10.1261/rna.035667.112
10. Chen LL, Yang L. Regulation of circRNA biogenesis. *RNA Biol*. 2015;12(4):381–388. doi:10.1080/15476286.2015.1020271
11. Wang F, Chen X, Han Y, et al. circRNA CDR1as regulated the proliferation of human periodontal ligament stem cells under a lipopolysaccharide-induced inflammatory condition. *Mediators Inflamm*. 2019;2019:1625381. doi:10.1155/2019/1625381
12. Xu Y, Yao Y, Zhong X, et al. Downregulated circular RNA hsa_circ_0001649 regulates proliferation, migration and invasion in cholangiocarcinoma cells. *Biochem Biophys Res Commun*. 2018;496(2):455–461. doi:10.1016/j.bbrc.2018.01.077

13. Hansen TB, Jensen TI, Clausen BH, et al. Natural RNA circles function as efficient microRNA sponges. *Nature*. 2013;495 (7441):384–388. doi:10.1038/nature11993
14. Harrandah AM, Mora RA, Chan EKL. Emerging microRNAs in cancer diagnosis, progression, and immune surveillance. *Cancer Lett*. 2018;438:126–132. doi:10.1016/j.canlet.2018.09.019
15. Braconi C, Huang N, Patel T. MicroRNA-dependent regulation of DNA methyltransferase-1 and tumor suppressor gene expression by interleukin-6 in human malignant cholangiocytes. *Hepatology*. 2010;51(3):881–890. doi:10.1002/hep.23381
16. Zou Y, Chen Z, He X, et al. High expression levels of unc-51-like kinase 1 as a predictor of poor prognosis in colorectal cancer. *Oncol Lett*. 2015;10(3):1583–1588. doi:10.3892/ol.2015.3417
17. Chen MB, Ji X-Z, Liu YY, et al. Ulk1 over-expression in human gastric cancer is correlated with patients' T classification and cancer relapse. *Oncotarget*. 2017;8(20):33704–33712. doi:10.18632/oncotarget.16734
18. Becker KF, Rosivatz E, Blechschmidt K, et al. Analysis of the E-cadherin repressor Snail in primary human cancers. *Cells Tissues Organs*. 2007;185(1–3):204–212. doi:10.1159/000101321
19. Xu Y, Yao Y, Liu Y, et al. Elevation of circular RNA circ_0005230 facilitates cell growth and metastasis via sponging miR-1238 and miR-1299 in cholangiocarcinoma. *Aging (Albany NY)*. 2019;11 (7):1907–1917. doi:10.18632/aging.101872
20. Liu P, Cui L, Shen L. Knockdown of TRIM52 alleviates LPS-induced inflammatory injury in human periodontal ligament cells through the TLR4/NF-kappaB pathway. *Biosci Rep*. 2020;40(8). doi:10.1042/BSR20201223
21. Hu D, Zhang Y. Circular RNA HIPK3 promotes glioma progression by binding to miR-124-3p. *Gene*. 2019;690:81–89. doi:10.1016/j.gene.2018.11.073
22. Wang X, Liang Z, Xu X, et al. miR-148a-3p represses proliferation and EMT by establishing regulatory circuits between ERBB3/AKT2/c-myc and DNMT1 in bladder cancer. *Cell Death Dis*. 2016;7(12): e2503. doi:10.1038/cddis.2016.373
23. Wang W, Dong J, Wang M, et al. miR-148a-3p suppresses epithelial ovarian cancer progression primarily by targeting c-Met. *Oncol Lett*. 2018;15(5):6131–6136. doi:10.3892/ol.2018.8110
24. Tiemin P, Peng X, Qingfu L, et al. Dysregulation of the miR-148a-GLUT1 axis promotes the progression and chemoresistance of human intrahepatic cholangiocarcinoma. *Oncogenesis*. 2020;9(2):19. doi:10.1038/s41389-020-0207-2
25. Dower CM, Bhat N, Gebru MT, et al. Targeted inhibition of ULK1 promotes apoptosis and suppresses tumor growth and metastasis in neuroblastoma. *Mol Cancer Ther*. 2018;17(11):2365–2376. doi:10.1158/1535-7163.MCT-18-0176
26. Hwang DY, Eom J-I, Jang JE, et al. ULK1 inhibition as a targeted therapeutic strategy for FLT3-ITD-mutated acute myeloid leukemia. *J Exp Clin Cancer Res*. 2020;39(1):85. doi:10.1186/s13046-020-01580-4
27. Tang F, Hu P, Yang Z, et al. SBI0206965, a novel inhibitor of Ulk1, suppresses non-small cell lung cancer cell growth by modulating both autophagy and apoptosis pathways. *Oncol Rep*. 2017;37 (6):3449–3455. doi:10.3892/or.2017.5555
28. Lv P, Lu F, Zhou WY, et al. miR-373 inhibits autophagy and further promotes apoptosis of cholangiocarcinoma cells by targeting ULK1. *Kaohsiung J Med Sci*. 2020;36(6):429–440. doi:10.1002/kjm2.12191